Journal of Magnetism and Magnetic Materials 446 (2018) 155–161

Contents lists available at ScienceDirect

Journal of Magnetism and Magnetic Materials

journal homepage: www.elsevier.com/locate/jmmm

Research articles

Linear magneto-viscoelastic model based on magnetic permeability components for anisotropic magnetorheological elastomers

I. Agirre-Olabide [a], P. Kuzhir [b], M.J. Elejabarrieta [a,*]

[a] Mech. & Manuf. Dept., Mondragon Unibertsitatea, 20500 Arrasate-Mondragon, Spain
[b] University Côte d'Azur, CNRS UMR 7010, Institute of Physics of Nice, Parc Valrose, 06100 Nice, France

ARTICLE INFO

Article history:
Received 30 July 2017
Accepted 7 September 2017
Available online 8 September 2017

Keywords:
Anisotropic magnetorheological elastomers
Magnetic permeability components
Fractional derivative model
Magneto-dynamic properties

ABSTRACT

A new magneto-viscoelastic model is presented for anisotropic magnetorheological elastomers (MREs), which combines the dynamic behaviour and magnetic permeability components. Five samples were synthesised with different particle contents. Dynamic properties were measured using a rheometer equipped with a magnetorheological cell. A four-parameter fractional derivative model was used to describe MRE viscoelasticity in the absence of a magnetic field. The magnetic permeability of each sample was measured with a vibrating sample magnetometer. From experimental measurements of longitudinal and transverse components of the magnetic permeability, the dependency with magnetic field was modelled. The new magneto-induced modulus model proposed in this work is based on the model developed by López-López et al. [19] for magnetorheological fluids, and was adapted for anisotropic MREs. The proposed model includes the longitudinal and transverse components of magnetic permeability, and it is valid for the linear viscoelastic region of anisotropic MREs. The errors between experimental values and the values predicted by the model do not exceed 10%. Hence, a new linear magneto-viscoelastic model for anisotropic MREs is developed, which predicts the effect of magnetic field on the dynamic shear modulus as a function of magnetic field intensity and frequency.

1. Introduction

Magnetorheological elastomers (MRE) consist of ferromagnetic particles embedded in an elastomeric matrix [1]. When an external magnetic field is applied to these materials, their mechanical properties are modified; and they are referred to as smart materials.

The properties of MREs are completely dependent on the particle distribution, which is therefore considered an important characteristic of MREs. Isotropic MRE samples are prepared by vulcanisation without an external magnetic field; these samples have a random particle distribution [2,3]. However, if an external magnetic field is applied during the vulcanisation process, the particles are aligned in the direction of the magnetic field, and consequently, particle chains or thicker chain aggregates are obtained; these samples are called anisotropic MREs [4,5].

Dynamic properties of anisotropic MREs are dependent on the matrix, particle content, and magnetic field. The predominant behaviour is the viscoelasticity, owing to the nature of the main component of these materials: silicone rubber or natural rubber [6,7]. This behaviour has been modelled for MRE materials by combining different elements such as dashpots and springs in different configurations [8,9]. To obtain a better fit to experimental data, more elements have been introduced by increasing the number of fitting parameters [10].

The fractional derivative model can be used to decrease the number of material parameters, and these parameters have a physical significance [11]. By using these advantages, the viscoelastic behaviour of isotropic [7,12] and anisotropic [13,14] MREs have recently been modelled using fractional derivative models. Agirre-Olabide et al. [12] used four material parameters to simulate the viscoelastic behaviour of isotropic MREs, and Xu et al. [7] combined a fractional Kelvin and Maxwell model in the parallel configuration to develop a higher order model (seven material parameters). Guo et al. [13] combined an Abel dashpot (fractional derivative element) and a spring in a series configuration, while Zhu et al. [14] employed a parallel configuration. Hence, three material parameters were used to predict the viscoelastic behaviour of anisotropic MREs.

The effect of the magnetic field on the properties of anisotropic MREs has been widely studied. Many models have assumed that perfectly aligned chains are created during the vulcanisation process. Jolly et al. [15,16] analysed the interaction of two particles by using dipole–dipole moments, while Davis [17] and Shen

* Corresponding author.
E-mail address: mjelejabarrieta@mondragon.edu (M.J. Elejabarrieta).

http://dx.doi.org/10.1016/j.jmmm.2017.09.017
0304-8853/

et al. [18] studied the interaction of each particle in the whole chain of particles. Bica et al. [4] used a dipolar magnetic moment approach and the ideal elastic body model.

López-López et al. [19] proposed a model for magnetorheological fluids by introducing the influence of aggregates having a body centered tetragonal (bct) internal structure (a more stable and more realistic structure), and they combined numerical simulations of the composite magnetic permeability with the analytical model predicting the stress–strain relationship. For MREs, Leng et al. [20] proposed an effective permeability model to estimate the shear storage modulus, and Dong et al. [21] developed a theoretical model for chains composed of magnetic particles and normal pressure, based on the effective permeability calculated by the Maxwell–Garnett mixing rule. Chen et al. [22] proposed a finite-column model to simulate the field-induced shear modulus.

The magnetic permeability of materials can be measured by using different techniques. De Vicente et al. [23] used a modified force balance method to measure the magnetic permeability of carbonyl iron powder suspension. Bellucci et al. [24] used vibrating sample magnetometry on a magnetic nanocomposite based on natural rubber. Schubert and Harrison [25] identified the permeability of isotropic and anisotropic MREs using an inverse modelling approach. Furthermore, they calculated the permeabilities of anisotropic MREs in the particle alignment direction and perpendicular to the alignment direction. However, de Vicente et al. [23] measured the permeability of carbonyl iron powder in a suspension and showed that the permeability decreases with the internal magnetic field.

A few magneto-viscoelastic models have been developed by coupling viscoelastic and magnetic interaction models. A classical four parameter magneto-viscoelastic model has been proposed by Li et al. [26], and all material parameters were fitted to experimental data for each magnetic field density. The magneto-viscoelastic behaviour using fractional derivatives has been modelled for isotropic [27] and anisotropic [13,14] MREs. Agirre-Olabide et al. [27] proposed a three-dimensional magneto-viscoelastic model within the linear viscoelastic region for isotropic MREs, by coupling a fractional-derivative-based viscoelastic model with a magnetic-field-dependant model. Conversely, the magneto-viscoelastic model proposed in [13,14] for anisotropic MREs is composed of a serial configuration a fractional derivative Maxwell model and a spring, which is dependent on the magnetic field and is modelled assuming chain-like structures. The strain amplitudes applied were 0.1% in [13] and 25% in [14], and the maximum magnetic field intensity was 300 mT.

In this work, we developed a new linear magneto-viscoelastic model for anisotropic MREs based on the longitudinal and transverse components of magnetic permeability. We modified the model developed by López-López et al. [19] for magnetorheological fluids, and we adapted it for anisotropic MREs. The new model assumes bulk column-like aggregates in the MR samples, and coupled it with the viscoelastic model. The viscoelastic model is based in a four-parameter fractional derivative model. We studied the influence of the magnetic field on the longitudinal and transverse components of the magnetic permeability of anisotropic MREs. We proposed a model to predict the evolution of the permeability components as a function of the external magnetic field (100–360 kA/m) and extend it for higher magnetic fields. The proposed new linear magneto-viscoelastic model was validated with experimental data, and can be extended to larger magnetic field and frequency conditions.

2. Experimental

In this work, anisotropic magnetorheological elastomers were synthesised using a room-temperature-vulcanising silicone rubber and soft magnetic particles; five particle contents were analysed. Two different characterisation techniques were performed; the dynamic behaviour was measured using a rheometer equipped with a magnetorheological device, and the magnetic properties were measured using a vibrating sample magnetometer (VSM).

2.1. Preparation of anisotropic samples

In this study, we used two components based on room-temperature-vulcanising vulcanised silicone rubber (RTV-SR): the main matrix WACKER Elastosil® M 4644A and the vulcaniser WACKER Elastosil® M 4644B mixed in a 10:1 ratio. The embedded soft magnetic spherical particles were carbonyl iron particles HS (BASF The Chemical Company, Germany) with a particle size of 1.25 ± 0.55 μm. Samples of five different particle volume fractions were prepared: 0%, 5%, 10%, 15%, and 20%.

The main matrix (Elastosil® M 4644A) and particles were mixed at the mentioned contents, and when a homogeneous mixture was obtained, the vulcaniser (Elastosil® M 4644B) was added. Every time a component was added, vacuum cycles for 30 min were applied to remove air bubbles generated during the mixing. Finally, the homogenous mixture was poured into a 1-mm-thick mould.

During the vulcanisation process, a magnetic field was applied in the thickness direction to obtain a chain alignment of the particles in the direction perpendicular to the shear strain applied during the rheometric experiments (Fig. 1). A magnetic field of a flux density of 130 mT was applied using a pair of permanent magnets placed on the both sides of the mould.

A Nova Nano SEM 450 scanning electron microscope (SEM) was used to observe the particle alignment and distribution (Fig. 2). The images were taken in a low vacuum condition with an acceleration voltage of 18 kV.

2.2. Magnetorheology

The dynamic properties of anisotropic MRE were measured using an Anton Paar Physica MCR 501 rheometer equipped with a MRD 70/1T magnetorheological cell, and a parallel plate configuration was used. To avoid slipping between the sample and plates, one of the plates had a serrated surface (PP20/MRD/TI/P2); a normal compressive force of 5 N was applied to the sample in order to increase the contact of the sample to the rheometer plates [28]. The sample's diameter and thickness were 20 mm and 1 mm, respectively. To check the reproducibility, three samples were studied for each particle content.

The samples were subjected to torsional deformation generated by a periodic oscillatory rotation of the upper rheometer plate. A strain amplitude of 0.01% was used in the frequency sweep tests to guarantee that all tests were performed in the linear viscoelastic

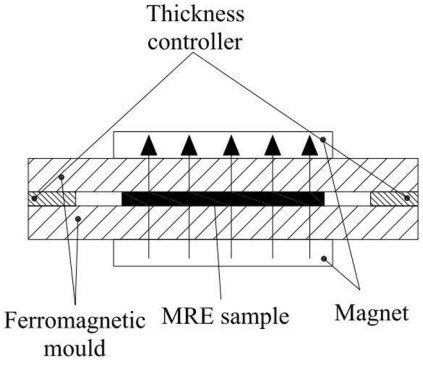

Fig. 1. Sketch of the anisotropic MRE sample vulcanisation device.

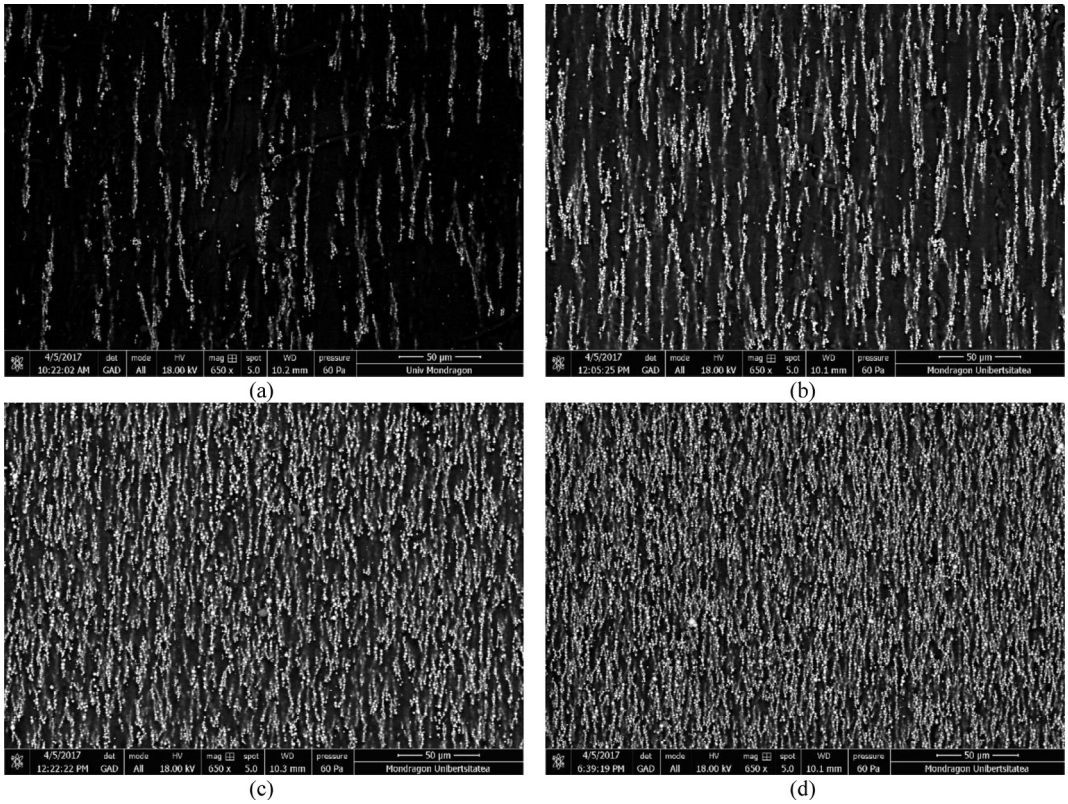

Fig. 2. SEM image of (a) 5%, (b) 10%, (c) 15%, and (d) 20% anisotropic RTV-SR MRE samples in low-vacuum conditions and with a voltage acceleration of 18 kV.

(LVE) region [29,30]. The frequency range of 0.1–40 Hz was analysed and divided into two steps: the first one from 0.1 to 10 Hz, and the second one from 10 to 40 Hz. In each step, 30 points were measured, while the acquisition time was fixed to 5 s per point. The temperature was controlled at 25 °C using the Julabo F-25 water-based heating/cooling system. Three magnetic field intensities were used: 0, 150, and 300 kA/m.

2.3. Vibrating sample magnetometer

The magnetostatic properties of the anisotropic MRE samples were investigated using a vibrating sample magnetometer (VSM, 4500 EG&G Princeton Applied Research). This technique consists of vibrating a sample at a frequency of 85 Hz in the direction perpendicular to a permanent and nearly homogeneous external magnetic field (Fig. 3). When a magnetic sample is introduced, it is magnetised and it consequently generates its own magnetic field around the sample. Periodic vibrations of the sample produce periodic variation of the magnetic field induced by the sample in the laboratory reference frame related to fixed electromagnets. According to Faraday's induction law, this change produces an electromotive force in the pick-up coils, which is measured and directly related to the sample magnetization.

All measurements were performed at room temperature in the field range of ± 360 kA/m. The aim of this characterisation was to measure the magnetic susceptibility of the sample in the direction parallel and perpendicular to the particle chains. For measurements of the longitudinal magnetic permeability, a sample with

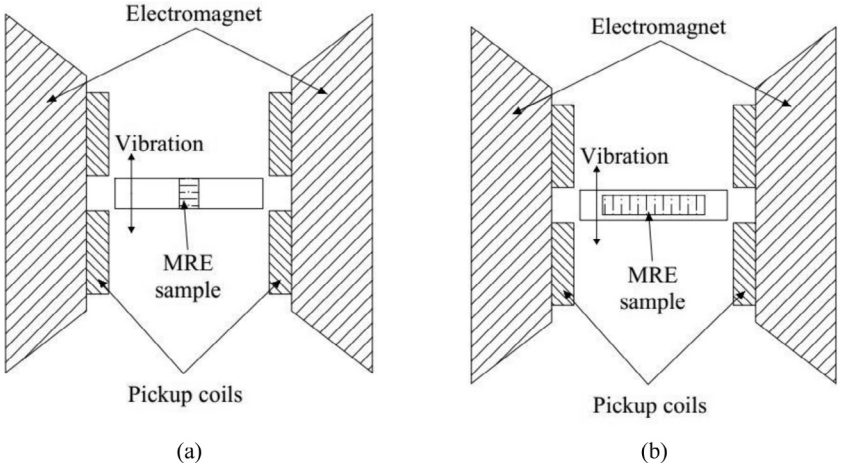

Fig. 3. VSM sketch for particles chains aligned in the (a) parallel and (b) perpendicular direction to the external magnetic field.

the chains oriented along the electromagnet axis and having a diameter of 3 mm and thickness of 1.08 ± 0.12 mm was used (Fig. 3(a)). For measurements of the transverse magnetic permeability, a sample with the chains oriented perpendicularly to the electromagnet axis and having a rectangular shape with a length of 10.48 ± 0.82 mm and thickness of 1 mm was used (Fig. 3(b)). These samples were held in an Ø3 × 20 mm container. One measurement was performed for each particle content.

From the VSM measurements, the longitudinal and transverse magnetic permeability of each sample was calculated for external fields from 100 to 360 kA/m.

3. Anisotropic MRE modelling

A four-parameter fractional derivative model was used, and the material parameters were identified using the dynamic properties measured by the rheometer. The influence of the magnetic field was introduced by using an empirical magneto-viscoelastic model [27] with the magnetic field contribution to the elastic modulus calculated using a variation of the model developed by López-López et al. [19] for magnetorheological fluids.

3.1. Fractional derivative model for MRE in the absence of the magnetic field

The generalised Zener model in the frequency domain written with fractional derivatives contains four parameters,

$$G^* = \frac{G_0 + (G_0 + C)(i\omega\tau)^\alpha}{1 + (i\omega\tau)^\alpha} = G_0 + \frac{C(i\omega\tau)^\alpha}{1 + (i\omega\tau)^\alpha}, \quad (1)$$

where G_0 is the static elastic modulus, $G_\infty = G_0 + C$ is the high frequency limit value of the dynamic modulus, τ is the relaxation time, and α is the fractional parameter [11,27], whose value varies between 0 and 1.

This model is applied to MRE samples in the absence of the field. In Fig. 4, experimental dynamic properties are shown as a function of frequency, and the error does not exceed the 5%. All samples show the same behaviour – both moduli increase with frequency and particle content.

After fitting Eq. (1) to the experimental data of each sample (Fig. 4), the four parameters of the fractional derivative model were obtained (table 1). The fitting was done using the least square method, and the minimised error was calculated for the shear complex modulus. The R^2 parameter is shown in order to evaluate the accuracy of the fitting.

Table 1
Fitting parameters of a four-parameter fractional derivative model for the anisotropic MRE samples and the R^2 parameter.

	G_0 (MPa)	C (MPa)	τ (s) [1 0 −7]	α	R^2
0%	0.120	0.157	152.1	0.253	0.997
5%	0.121	0.198	95.23	0.229	0.971
10%	0.131	0.212	51.72	0.224	0.993
15%	0.138	0.379	5.919	0.180	0.965
20%	0.148	0.467	6.863	0.172	0.987

Fig. 4 shows the fitting and the experimental results. The fitting is accurate for all contents in the studied frequency band. However, the fitting is better for the storage modulus than for the loss modulus because the storage modulus is one order of magnitude higher than the loss modulus, and consequently, its influence on the complex modulus is larger. The larger mean relative error does not exceed 0.5% for the storage modulus and 6% for the loss modulus.

3.2. Magnetic field effect

The dynamic properties of anisotropic MREs increase with magnetic field intensity (Fig. 5), and a larger increase was measured with a larger magnetic field.

In this study, we assumed that the magnetic field only modifies G_0 and C parameters (Eq. (1)). Consistency of this assumption has been proved in [27]. These parameters are supposed to depend on the magnetic field density (H) and the volumetric particle content (φ), as follows:

$$G_0(\varphi, H) = G_0 + \Delta C(\varphi, H) \text{ and } C(\varphi, B) = \Delta C(\varphi, H), \quad (2)$$

where G_0 and C corresponds to the fitting values of each particle content (Table 1), and ΔC is the elastic modulus variation due to the external magnetic field. The magnetic field (ΔC) and the viscoelastic model were coupled as follows:

$$G^* = (G_0 + \Delta C) + \frac{(C + \Delta C)(i\omega\tau)^\alpha}{1 + (i\omega\tau)^\alpha}. \quad (3)$$

The López-López et al. model [19] was used for magnetorheological fluids in order to introduce the influence of aggregates generated when an external magnetic field was applied. This model assumes bulk-column-like aggregates in the MR sample extended along the applied magnetic field – a more stable and more realistic structure observed in experiments for both MR fluids and MRE. Moreover, the model was analysed for a magnetic field intensity

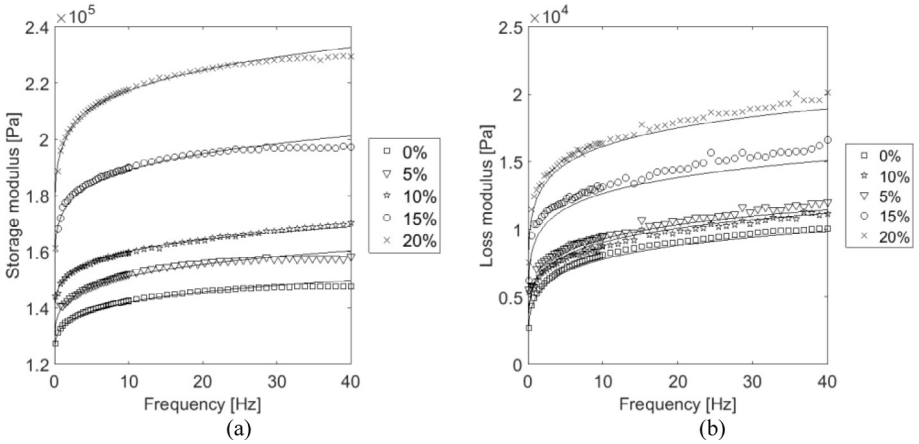

Fig. 4. Dynamic properties of anisotropic MRE samples as a function of frequency, (a) storage and (b) loss modulus. Experimental data are represented as points, and the lines correspond to the fitting of Eq. (1).

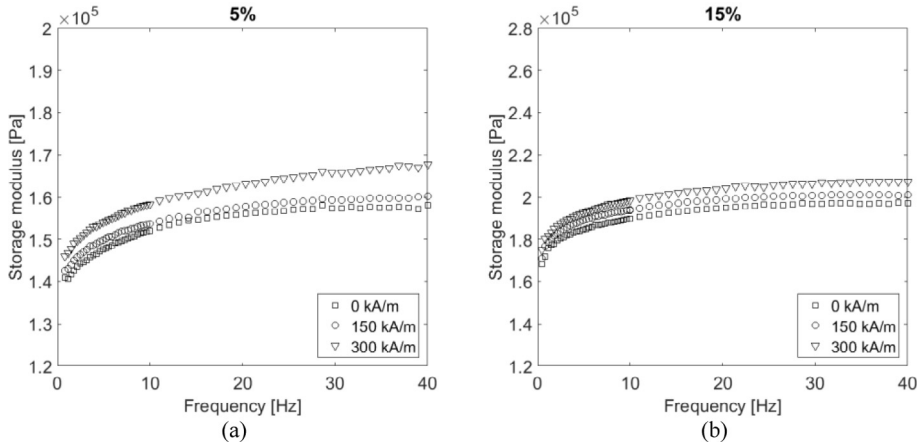

Fig. 5. Influence of the magnetic field on the MRE storage modulus for (a) 5% and (b) 15% anisotropic MRE samples as a function of frequency.

of 18.5 kA/m and a volumetric particle content of 50%. The model is based on the evaluation of the free energy of the sheared MR sample, and the shear stress σ is related to the applied strain γ, as follows:

$$\sigma = \mu_0 H^2(\mu_\parallel - \mu_\perp)\frac{\gamma}{(1+\gamma^2)} - \frac{1}{2}\mu_0 H^2\left[\frac{\partial\mu_\parallel}{\partial\gamma}\cdot\frac{1}{1+\gamma^2} + \frac{\partial\mu_\perp}{\partial\gamma}\cdot\frac{\gamma^2}{1+\gamma^2}\right] + \frac{1}{2}\mu_0 H^2(\mu_\parallel - \mu_\perp) \times \frac{\gamma}{1+\gamma^2} \quad (4)$$

where H is the magnetic field intensity within the samples, and $\mu_\parallel$ and $\mu_\perp$ are the longitudinal and transverse components of the magnetic permeability; the second term containing magnetic permeability derivatives appears to be negligible at strong magnetic fields used in our rheological experiments, so it is neglected. Moreover, MR fluids operate within a post-yield continuous shear or flow regime, while MREs operate in the pre-yield region [31], which means that the strain amplitudes applied to MREs are smaller. After linearization of Eq. (4), the following expression was developed,

$$\Delta C = \frac{3}{2}\mu_0\left(\frac{H_0}{\mu_\parallel}\right)\mu_\parallel - \mu_\perp, \quad (5)$$

where ΔC is the increment of the zero-frequency storage modulus due to internal magnetic field, $H = H_0/\mu_\parallel$, and H_0 is the applied external magnetic field. From the magnetization measurements (Section 2.3), the influence of the magnetic field on the permeability properties was studied. The longitudinal and transverse magnetic permeability components decrease linearly with the external magnetic field (Fig. 6). The permeability is larger for high particle content and for lower magnetic fields, and the longitudinal one is larger than the transverse one owing to the lower demagnetizing effect in the sample with the aggregates oriented along the applied field. Moreover, the magnetic permeability decrease is larger for the longitudinal component and particle content. Therefore, we propose to use a linear equation (Eq. (6)) fitting for each component and particle content, which are shown in Fig. 6, and the R^2 was higher than 0.963 for all the cases,

$$\mu_\parallel(H,\phi) = -a_{\parallel,\phi}\,(H-100) + \mu_{\parallel,\phi}$$
$$\mu_\perp(H,\phi) = -a_{\perp,\phi}\,(H-100) + \mu_{\perp,\phi} \quad (6)$$

where $a_{\parallel,\varphi}$ and $a_{\perp,\varphi}$ are the slope values of permeability components for each particle content, $\mu_{\parallel,\varphi}$ and $\mu_{\perp,\varphi}$ are the permeability components at 100 kA/m for each particle content, and H is in kA/m. As an example, $a_{\parallel,5\%}$ corresponds to the slope of longitudinal component of the 5% sample and $\mu_{\perp,5\%}$ to the transverse component of the 5% sample at 100Fig. 7 kA/m.

From Fig. 6, the longitudinal and transverse components of magnetic permeability at 150 and 300 kA/m are substituted in Eqs. (5) and (6), and introduced in (3). As can be seen in Fig. 7, after including the modelling of magnetic permeability components, the

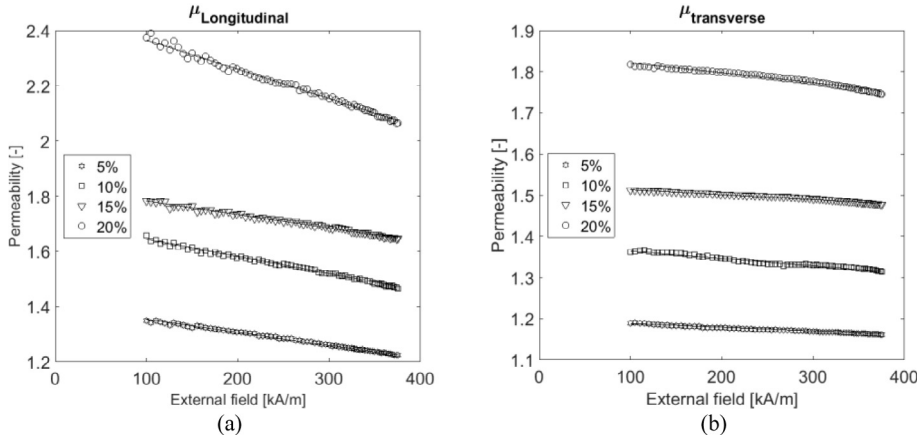

Fig. 6. (a) Longitudinal and (b) transverse components of the magnetic permeability of anisotropic MRE samples. Experimental data are represented as points, and the lines correspond to the fitting.

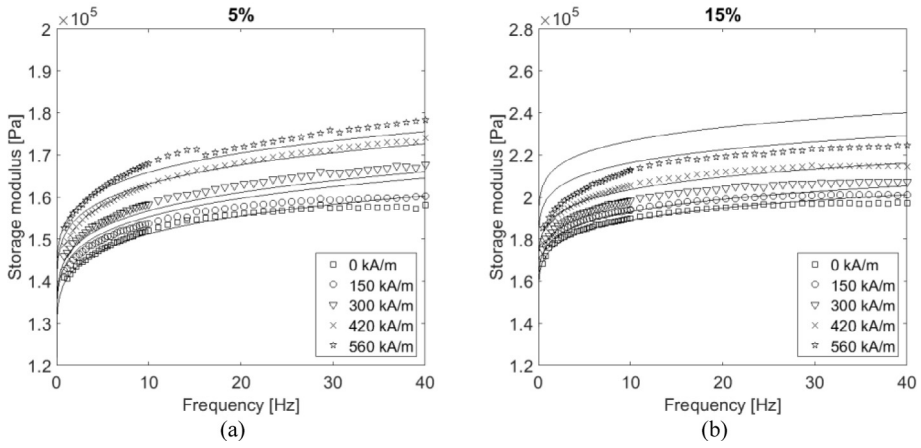

Fig. 7. Influence of magnetic field for (a) 5% and (b) 15% anisotropic MRE samples as a function of frequency for the coupling of Eqs. (3), (5), and (6). 150 and 300 kA/m curves are modelled using experimental data, and the 420 and 560 kA/m curves are the extension of the proposed model.

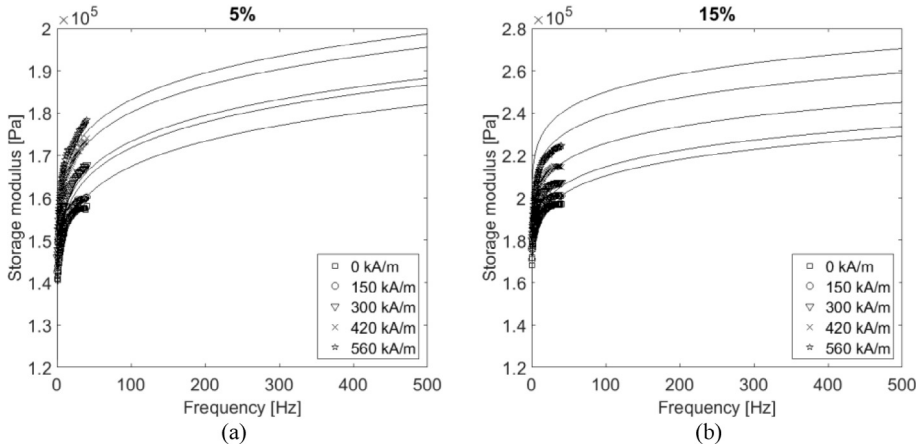

Fig. 8. Extension of the proposed new model in the frequency domain. Storage modulus of (a) 5% and (b) 15% anisotropic MRE samples.

predicted behaviour is similar — the discrepancy does not exceed 8%.

Magnetic permeability components are modelled as a function of external magnetic field, and consequently magnetic field higher than experimental ones can be predicted. In Fig. 7, we extended the model developed in this work for 420 and 560 kA/m. For low particle contents, the discrepancy is lower than 7% at high magnetic fields, while at high magnetic field and particle contents, it does not exceed 10%. Furthermore, the proposed model can also be modelled in the frequency domain, as shown in Fig. 8, which does not affect the error.

4. Conclusions

In this work, a new magneto-viscoelastic model is proposed for anisotropic MREs within the lineal viscoelastic region, which can be extended in the frequency and magnetic field domain. The four-parameter fractional derivative viscoelastic model was successfully fitted to experimental data of anisotropic MREs samples in the absence of the applied field. The mean fitting errors does not exceed the 1% for the storage modulus and 6% for the loss modulus.

The viscoelastic model for anisotropic MREs was coupled with the magneto-induced modulus model (based on the López-López model). The proposed magnetic model was fed with the longitudinal and transverse components of magnetic permeability of the samples.

The longitudinal and transverse components of magnetic permeability of anisotropic MREs has been measured and modelled in the magnetic field domain. The VSM measurements were performed, and experimental data were introduced for the coupled model. The model prediction was compared with rheological measurements, and the discrepancy does not exceed the 7%. Both components decrease with magnetic field, and the decreases are larger with particle content and longitudinal component. Moreover, the permeability values increase with particle content.

The new model can be extended in the magnetic field domain, in order to overcome VSM limitations (maximum magnetic field intensity of 360 kA/m). The model was extended for 420 and 560 kA/m fields, while the discrepancy is smaller than 10%.

Hence, a new magneto-viscoelastic model for anisotropic MREs is proposed by coupling a four-parameter fractional derivative model with the magnetic model, including the components of magnetic permeability. Moreover, the model can be extended in the frequency and magnetic field domain, which overcomes the experimental limitations, 40 Hz and 360 kA/m.

Acknowledgements

The authors gratefully acknowledge the financial support from the Department of Education of the Basque Government for the

Research Predoc Grant PRE_2014_1_284 and PI-2016-1-0026 research project; and DPI 2015-71198-R research project from the Spanish Government.

Appendix A. Supplementary data

Supplementary data associated with this article can be found, in the online version, at http://dx.doi.org/10.1016/j.jmmm.2017.09.017.

References

[1] L.A. Makarova, Y.A. Alekhina, N.S. Perov, Peculiarities of magnetic properties of magnetoactive elastomers with hard magnetic filler in crossed magnetic fields, J. Magn. Magn. Mater. 440 (2017) 30–32.
[2] N.A. Yunus, S.A. Mazlan, S. Ubaidillah, F. Imaduddin Choi, S.A. Abdul Aziz, et al., Rheological properties of isotropic magnetorheological elastomers featuring an epoxidized natural rubber, Smart Mater. Struct. 25 (2016) 107001, http://dx.doi.org/10.1088/0964-1726/25/10/107001.
[3] W. Gao, X. Wang, Steady shear characteristic and behavior of magneto-thermo-elasticity of isotropic MR elastomers, Smart Mater. Struct. 25 (2016) 25026, http://dx.doi.org/10.1088/0964-1726/25/2/025026.
[4] I. Bica, M. Balasoiu, A.I. Kuklin, Anisotropic silicone rubber based magnetorheological elastomer with oil silicone and iron microparticles, Solid State Phenom. 190 (2012) 645–648, http://dx.doi.org/10.4028/www.scientific.net/SSP.190.645.
[5] S. Aloui, M. Klüppel, Magneto-rheological response of elastomer composites with hybrid-magnetic fillers, Smart Mater. Struct. 24 (2015) 25016, http://dx.doi.org/10.1088/0964-1726/24/2/025016.
[6] H.S. Jung, S.H. Kwon, H.J. Choi, J.H. Jung, Y.G. Kim, Magnetic carbonyl iron/natural rubber composite elastomer and its magnetorheology, Compos. Struct. 136 (2016) 106–112, http://dx.doi.org/10.1016/j.compstruct.2015.10.008.
[7] Z.D. Xu, Y.X. Liao, T. Ge, C. Xu, Experimental and theoretical study of viscoelastic dampers with different matrix rubbers, J. Eng. Mech. 142 (2016) 4016051, http://dx.doi.org/10.1061/(ASCE)EM.1943-7889.0001101.
[8] L. Chen, S. Jerrams, A rheological model of the dynamic behaviour of magnetorheological elastomers, J. Appl. Phys. 13513 (2011) 1–9, http://dx.doi.org/10.1063/1.3603052.
[9] M. Behrooz, X. Wang, F. Gordaninejad, Modeling of a new semi-active/passive magnetorheological elastomer isolator, Smart Mater. Struct. 23 (2014) 45013, http://dx.doi.org/10.1088/0964-1726/23/4/045013.
[10] G. Zhu, Y. Xiong, S. Daley, R. Shenoi, Magnetorheological elastomer materials and structures with vibration energy control for marine application, in: Anal. Des. Mar. Struct. V, CRC Press, 2015, pp. 197–204, http://dx.doi.org/10.1201/b18179-27.
[11] T. Pritz, Analysis of four-parameter fractional derivative model of real solid materials, J. Sound Vib. 195 (1996) 103–115, http://dx.doi.org/10.1006/jsvi.1996.0406.
[12] I. Agirre-Olabide, M.J. Elejabarrieta, Maximum attenuation variability of isotropic magnetosensitive elastomers, Polym. Test. 54 (2016) 104–113, http://dx.doi.org/10.1016/j.polymertesting.2016.06.021.
[13] F. Guo, C.-b. Du, R.-p. Li, Viscoelastic parameter model of magnetorheological elastomers based on Abel Dashpot, Adv Mech. Eng. 6 (2015), http://dx.doi.org/10.1155/2014/629386, 629386–629386.
[14] J. Zhu, Z. Xu, Y. Guo, Experimental and modeling study on magnetorheological elastomers with different matrices, J. Mater. Civ. Eng. 25 (2013) 1762–1771, http://dx.doi.org/10.1061/(ASCE)MT.1943-5533.0000727.
[15] M.R. Jolly, J.D. Carlson, B.C. Muñoz, T.A. Bullions, The magnetoviscoelastic response of elastomer composites consisting of ferrous particles embedded in a polymer matrix, J. Intell. Mater. Syst. Struct. 4 (1996) 613–622, http://dx.doi.org/10.1177/1045389X9600700601.
[16] M.R. Jolly, J.D. Carlson, B.C. Muñoz, A model of the behaviour of magnetorheological materials, Smart Mater. Struct. 5 (1999) 607–614, http://dx.doi.org/10.1088/0964-1726/5/5/009.
[17] L.C. Davis, Model of magnetorheological elastomers, J. Appl. Phys. 85 (1999) 3348–3351, http://dx.doi.org/10.1063/1.369682.
[18] Y. Shen, M.F. Golnaraghi, G.R. Heppler, Experimental research and modeling of magnetorheological elastomers, J. Intell. Mater. Syst. Struct. 15 (2004) 27–35, http://dx.doi.org/10.1177/1045389X04039264.
[19] M.T. López-López, P. Kuzhir, J. Caballero-Hernández, L. Rodríguez-Arco, J.D.G. Duran, G. Bossis, Yield stress in magnetorheological suspensions near the limit of maximum-packing fraction, J. Rheol. 56 (2012) 1209, http://dx.doi.org/10.1122/1.4731659.
[20] D. Leng, L. Sun, J. Sun, Y. Lin, Derivation of stiffness matrix in constitutive modeling of magnetorheological elastomer, J. Phys. Conf. Ser. 412 (2013) 12028, http://dx.doi.org/10.1088/1742-6596/412/1/012028.
[21] X. Dong, N. Ma, J. Ou, M. Qi, Predicating magnetorheological effect of magnetorheological elastomers under normal pressure, J. Phys. Conf. Ser. 412 (2013) 12035, http://dx.doi.org/10.1088/1742-6596/412/1/012035.
[22] L. Chen, X.L. Gong, W.H. Li, Microstructures and viscoelastic properties of anisotropic magnetorheological elastomers, Smart Mater. Struct. 16 (2007) 2645–2650, http://dx.doi.org/10.1088/0964-1726/16/6/069.
[23] J. de Vicente, G. Bossis, S. Lacis, M. Guyot, Permeability measurements in cobalt ferrite and carbonyl iron powders and suspensions, J. Magn. Magn. Mater. 251 (2002) 100–108, http://dx.doi.org/10.1016/S0304-8853(02)00484-5.
[24] F.S. Bellucci, F.C. Lobato de Almeida, M.A. Lima Nobre, M.A. Rodrgíuez-Pérez, A. T. Paschoalini, A.E. Job, Magnetic properties of vulcanized natural rubber nanocomposites as a function of the concentration, size and shape of the magnetic fillers, Compos. Part B Eng. 85 (2016) 196–206, http://dx.doi.org/10.1016/j.compositesb.2015.09.013.
[25] G. Schubert, P. Harrison, Magnetic induction measurements and identification of the permeability of magneto-rheological elastomers using finite element simulations, J. Magn. Magn. Mater. 404 (2016) 205–214, http://dx.doi.org/10.1016/j.jmmm.2015.12.003.
[26] W.H. Li, Y. Zhou, T.F. Tian, Viscoelastic properties of MR elastomers under harmonic loading, Rheol. Acta 49 (2010) 733–740, http://dx.doi.org/10.1007/s00397-010-0446-9.
[27] I. Agirre-Olabide, A. Lion, M.J. Elejabarrieta, A new three-dimensional magneto-viscoelastic model for isotropic magnetorheological elastomers, Smart Mater. Struct. 26 (2017) 35021, http://dx.doi.org/10.1088/1361-665X/26/3/035021.
[28] X. Dong, N. Ma, M. Qi, J. Li, R. Chen, J. Ou, The pressure-dependent MR effect of magnetorheological elastomers, Smart Mater. Struct. 21 (2012) 75014, http://dx.doi.org/10.1088/0964-1726/21/7/075014.
[29] I. Agirre-Olabide, J. Berasategui, M.J. Elejabarrieta, M.M. Bou-Ali, Characterization of the linear viscoelastic region of magnetorheological elastomers, J. Intell. Mater. Syst. Struct. 25 (2014) 2074–2081, http://dx.doi.org/10.1177/1045389X13517310.
[30] I. Agirre-Olabide, M.J. Elejabarrieta, M.M. Bou-Ali, Matrix dependence of the linear viscoelastic region in magnetorheological elastomers, J. Intell. Mater. Syst. Struct. 26 (2015) 1880–1886, http://dx.doi.org/10.1177/1045389X15580658.
[31] J.D. Carlson, M.R. Jolly, MR fluid, foam and elastomer devices, Mechatronics 10 (2000) 555–569, http://dx.doi.org/10.1016/S0957-4158(99)00064-1.